

Original Research Article

GREEN SYNTHESIS OF ZINC OXIDE NANOPARTICLES USING *Colocasia esculenta* TUBER PEEL EXTRACT: CHARACTERIZATION AND ANTIMICROBIAL STUDIES AGAINST WHITE YAM PATHOGENS

ABSTRACT

Aims: To biosynthesize and characterize Zinc Oxide NPs using *Colocasia esculenta* (Cocoyam) tuber peel extract as well as explore its antimicrobial potential against white yam pathogens.

Place and Duration of Study: Sample: Department of Biological Sciences, Benue State University, Makurdi, and November, 2022.

Methodology: The method described by Nakade (2013) was used for phytochemical analysis (Tanins, Saponins, Flavonoids, Alkaloids, Steroids, Quinones, Starch, Terpenoids and Glycosides). The biosynthesized ZnO NPs were characterized by UV-Visible, XRD, SEM, EDX and FTIR.

Antimicrobial sensitivity test was by the method of (Shiriki., et al, 2017) was employed with slight modification.

Results: Optimization studies revealed that the maximum rate of synthesis could be achieved with 0.50 M ZnO solution at 90 °C in 5 hours. The study revealed ZnO NPs that are crystalline with hexagonal shapes. The average crystallite size was 10 nm with a range of 7.81 nm- 9.23 nm. FTIR spectra of the tuber peel extract and the synthesized ZnO NPs revealed reducing, capping and stabilizing agents such as amines, peptides, amides and phenolic groups. The biosynthesized ZnO NPs exhibited antimicrobial action in a dose-dependent manner against five white yam pathogenic fungi: *Aspergillus niger*, *Botryodiplodia theobromae*, *Zygosaccharomyces bailli*, *Zygosaccharomyces rouxii* and *Myrothecium verrucaria* as well as three bacteria: *Klebsiella oxytoca*, *Serratia marcescens* and *Pseudomonas aeruginosa*.

Conclusion: The biosynthesized ZnO NPs exhibited slightly to moderate and effective inhibition ranging from 15.54 %- 98.52 % on the test organisms when compared with standard antifungal (Fluconazole) and antibacterial (Ciprofloxacin) agents.

Keywords: Phytochemicals, nanotechnology, biosynthesis, pathogens, antimicrobial activity.

Commented [2A1]: Spelling error here

1. INTRODUCTION

Nanotechnology is an area with the objective of facilitating the manufacture of nanomaterials or nanoparticles by the manipulation of matter through physical, chemical, or biological processes to create materials with specific properties, which can be used in particular applications (Jayanta et al., 2020). Green nanotechnology emphasizes simple work-up procedures for the synthesis of reusable, cost effective, and eco-friendly nanoparticles with sustainable commercial viability.

The term "nanomaterials" is defined by the European Commission (EC) and the International Organization Standards (ISO) as a subgroup of nano-objects, and their agglomerates (weakly bonded, embedded) and aggregates (strongly bonded, fixed) (Josef et al., 2015). They are the conventional materials which are consciously and deliberately engineered to nanostructure of modern application of nanotechnology. Nanomaterials are the forms of matter with at least one of their dimensions ranging from 1 to 100 nm. **Nonamaterials** have found wide applications in agriculture, medicine, pharmaceutical, electrical and electronics, cosmetics, textile, paint, ceramics, rubber, water purification and environmental remediation.

Commented [2A2]: Spelling error here

Generally, there are two approaches to the preparation of nanoparticles: top-down and bottom-up approaches. In top-down methods, NPs can be produced by the division of a massive solid into smaller portions (nanosize). The bottom-up method of NPs preparation involves building up from atoms or molecular entities to nanometric scale (Josef et al., 2015). The bottom-up approaches give better nanoparticles with little or no defects (Jayanta, 2020).

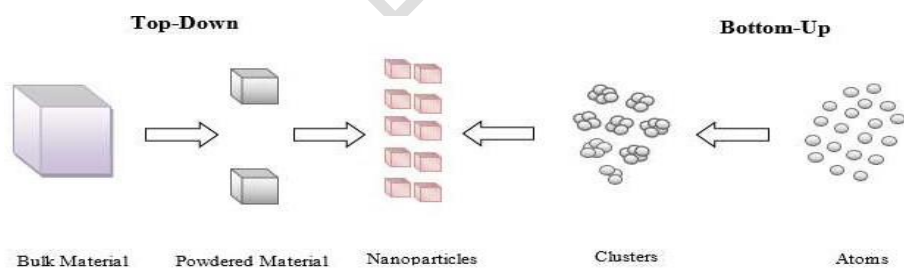


Figure1: Approaches for the synthesis of nanoparticles (Josef et al., 2015)

Physical, chemical and biological methods are employed for the synthesis of NPs. However, physical and chemical methods are associated with high-energy demand, sometimes generating toxic wastes with the attendant health and environmental consequences (Gunalan. et al., 2012). Compared to physical and chemical routes for the synthesis of NPs, biological methods are simple, efficient, cost effective, eco-friendly, non-toxic and often lead to large scale production,

formation of purer and stable nanoparticles with relatively mild operating conditions (Mittal et al., 2013; Kharissova., et al., 2013; Parveen et al., 2016).

Biological or green synthesis of nanoparticles which, represents a connection between biotechnology and nanotechnology has received increasing consideration due to the growing need to develop environmentally friendly technologies for material synthesis. Recently, considerable efforts are directed at exploring the potentials of plant extracts for the synthesis of NPs as alternative to synthetic chemicals for various applications. These plant extracts are rich in phytochemicals such as alkaloids, flavonoids, terpenoids, phenols, glycosides, tannins, phytates, saponins, steroids etc with proven antimicrobial actions serve as reducing, capping and stabilizing agents during synthesis (Nakade et al., 2013).

Several metals and metal oxides such as iron, nickel, silver, gold, aluminum, copper, iron oxide, copper oxide, zinc oxide, titanium dioxide and silicon oxide etc are known sources of nanomaterials. Among the metal oxide, ZnO is one of the most widely used NPs owing to its excellent antimicrobial properties, non-toxicity, good Ultraviolet (UV) absorbance, high stability (only decomposing into zinc vapour and oxygen at around 1975 °C), and photocatalytic attributes (Yasser & Nassim, 2019). ZnO is also a food supplement and is considered as a safe material for human beings by the United States Food and Drug Administration (US FDA) (Yasser & Nassim; 2019; Zare. et al., 2017). The unique Physical, chemical and mechanical properties of ZnO permits its wide applications in the production of pharmaceuticals, cosmetics, electronics, cement, glass, paints, automobile tyres and fabricated rubber products, plumbing fixtures, glue, tiles, ceramics and porcelains, feed additives, seed treatment, inks, electrostatic copying paper and colour photography, flame retardants, semiconductor manufacturing and ultraviolet absorbers in plastics as well as in medical, optical, biologics, photonics, water purification, and environment remediation etc (Yasser and Nassim, 2019). ZnO has a potential biocompatibility over many metal oxides (Zare et al., 2017).

Cocoyam or Taro (*Colecosia esculenta* L) is a herbacious tropical perennial starchy plant that is rich in phytochemicals such as alkaloids, flavonoids, terpenoids, phenols, glycosides, tannins, phytates, saponins, steroids etc with antifungal, antibacterial and antiviral properties (Eleazu, 2016). The crop is of great nutritional and economic importance to humankind. The leaves are used as vegetables and are a rich source of proteins, ascorbic acid, dietary fibre, minerals and vitamins such as calcium, phosphorus, iron, magnesium, potassium, vitamin C, thianine, ribboflavin and niacin. The leaves juice is applied over scorpion sting or snake bite for treatment (Wang, 2012). The tubers are rich in starch and the corns contain the anthocyanins, cyanidin, glucoside, pelargadin, 3-glycoside, and 3-rhamnoside (Eleazu, 2016). The related anthocynin with flavonoids are reported to improve blood circulation by decreasing capillary fragility, improve eye sight, acts as potent antioxidant, anti-inflammatory and anti-cancer agents (Wang, 2013;; Nakade., et al, 2013). The corns

also contain calcium oxalate, an irritant that prevents them being eaten raw or incompletely cooked (Nakade., et al, 2013). In ethno-medicine, *C. esculenta* tuber is used in the management of diabetes mellitus, treatment of ringworm, cough, sore throat and wounds (Pritha., et al, 2015) and has been reported to have antihelminthic and anticancer properties (Nakade et al., 2013; Pritha et al, 2015) These biological properties are because of its phytochemicals.

Several studies have supported the synthesis of ZnO NPs from various plant parts like leaf, flower, seed, fruit, root, rhizome, stem, bark, and peel extracts (Zare et al, 2017; Lakshuni et al., 2012). For example, studies by many researchers utilized leaf extracts of *Ocimum basilium* [(Salam., et al, 2015)], *Aleo barbadensis* (Sangeetha et al., 2011), *Plectranthus amboinicus* (Vilayakumar et al., 2015), *Azadirachta indica* L (Elumalai & Velmurugan, 2015), *Couroupita guineensis* (Aathishkumar.et al., 2017) ,*Hibiscus rosa-sineensis* (Divya et al., 2013) etc; flower extracts of *Cassia auriculata* (Ramesh., et al, 2014); seed extracts of *Cuminum cyminum* *Pongamia pinnata* (Zare., et al, 2017), fruit extracts of *Emblca officinalis*, *Borassus flabellifer*,*Artocarpus gomezianus* and orange juice (Jha., et al, 2011); root extracts of *Rubus fairholmianus*, *Withania somnifera* (Zare.et al., 2017); rhizome extracts of *Zingiber officinale*,*Bergenia ciliate* (Zare, 2017; Liu, 2001), stem extracts of *Phyllanthus embilica*, bark extracts of *Cinnamomum verum*, *Albizia lebbbeck* (Pritha. et al., 2015), *gum kayara* (Padil & Cernik, 2013) as well as peel extracts of *rubantan* (Rajiv., et a, 2013), *Punica granatum*, *Musa sapientum* (Pritha. et al., 2015; Zare et al., 2017).

Several factors such as pH, temperature, concentration of precursor and volume of extract can influence nanoparticle synthesis and its resulting characteristics (Moloto et al., 2009). Morphology and particle size are controlled by precursor concentration and volume ratio of precursor-extract used (Sibiya & Moloto, 2014; Amin. et a.l, 2011). This research to biosynthesis and characterizes ZnO NPs using *C. esculenta* tuber peel extract as well as explores its antimicrobial potential against white yam pathogens.

2. MATERIAL AND METHODS

Previously isolated and identified white yam rot pathogens comprising of five fungi: *Aspergillus niger*, *Botrydioplodia theorome*, *Zygosaccharomyces bailli* and *Zygosaccharomyces rouxil* and *Myrothecium verrucaria* and three bacteria: *Klebsiella oxytoca*, *Serratia marcescens* and *Pseudomonas aeruginosa* of 2022 harvest year were obtained from the Laboratory, Department of Biological Sciences, Benue State University, Makurdi where they were preserved and used for the antimicrobial study. *C. esculenta* tubers were purchased from Railway market, Makurdi, Benue State, properly labeled, packed in clean cellophane bags and transported to the Department of Botany, Benue State University, Makurdi for authentication by a plant taxonomist. ZnO was purchased from Agbe Sciences, Makurdi, Benue State, Nigeria. All

Commented [2A3]: Prepare a flowchart.

reagents used were analytical grade and used as received without further purification. All solutions were freshly prepared using double-distilled water and kept in the dark to avoid photochemical reactions. All glassware used in the experimental procedures were sterilized in 10 % sodium hypochlorite solution, rinsed thoroughly in double-distilled water and dried before use. Aseptic condition was maintained throughout the experiments.

2.1 PLANT EXTRACT PREPARATION

The *C. esculenta* tubers were thoroughly washed with sterile water, peeled and dried in the shade for two weeks to avoid chemical decomposition. Upon drying, the peels were made into fine powder using a wooden mortar and pestle.

2.2 EXTRACTION PROCEDURE

The method described by Shiriki et al., (2019) was employed with little modification. The sample (500 g) was packed into the thimble and placed inside the extractor. 800 mL methanol was put in the round bottom flask of the extractor and heated on a heating mantle for 8 hours. After extraction, the methanol was recovered and the extract evaporated in a beaker to a constant weight over an evaporation bath for 24 hours. The sample was then weighed and the yield calculated in percentage. The extract was kept in the refrigerator for further analysis.

2.3 PHYTOCHEMICAL ANALYSIS

The method described by Nakade (2013) was used for phytochemical analysis.

i. Test for tannins

Ferric Chloride Test: 4 mL of the extract was treated with 4 mL of FeCl_3 in a test tube. Formation of a bluish green precipitates indicated the presence of tannins.

ii. Test for Saponins

Froth Test : 5 mL of the extract was diluted to 20 mL with distilled water and shaken in a graduated cylinder for 15 minutes. Formation of 1 cm layer of foam indicated the presence of saponins.

iii. Test for flavonoids

Lead Acetate Test: 1 mL of 5 % lead acetate solution was added to 1 mL of the extract solution in a test tube and the mixture was allowed to stand for five minutes. The formation of precipitate in the mixture confirmed the presence of flavonoids.

iv. Test for Phenols

Ferric Chloride Test: 3 drops of ferric chloride solution was added to 1 mL of the extract in a test tube. The appearance of bluish-black colour indicates the presence of phenols.

v. Test for alkaloids

Hager's Test: 5 mg of the extract was dissolved in 3 mL of with dilute Hydrochloric acid and filtered. 2 mL of the filtrate was treated with Hager's reagent (saturated picric acid solution) in a test tube. The formation of yellow precipitates confirmed the presence of alkaloids.

vi. Test for steroids

Libermann Burchard's Test: 2 mL of the extract was treated with 2 mL of acetic anhydride and a drop of acetic acid, heated for 5 minutes and cooled in ice followed by addition of 1 mL of concentrated tetraoxosulphate (vi) acid carefully by the sides of the test tube. An array of colours changes from violet to blue or green indicated the presence of steroids.

vii. Test for quinones

Hydrochloric Acid Test: 1 mL of the extract was treated with 3 drops of concentrated hydrochloric acid. A green colour indicated the presence of quinones.

viii. Test for starch

Iodine Test: 1 mL of the extract was treated with 3 drops of iodine solution. A blue-black colour or dark blue colour indicated the presence of starch.

ix. Test for terpenoids

Salkowski Test: 5 mL of the extract was treated with 2 mL chloroform, followed by 3 mL of concentrated tetraoxosulphate (vi) acid to form a layer. A redish brown interface indicated the presence of terpenoids.

x. Test for glycosides

Keller- Killani Test: 5 mL of the extract was be treated with 2 mL glacial acetic acid, followed by a drop of FeCl_3 solution and then 1 mL of concentrated tetraoxosulphate (vi) acid. Violet green rings appearing below the brown ring in the acetic acid layer indicated a positive test for glycosides.

2.4 SYNTHESIS OF ZINC OXIDE NANOPARTICLES (ZNO NPS)

The method described by *Farjana et al, 2022* was used with slight modification. 10 mL aqueous 0.50 mol dm^{-3} ZnO was mixed with 5 mL of the extract in a 250 mL beaker. Then, the pH of the solution was adjusted to 12 by a drop-wise addition of 0.02 mol dm^{-3} aqueous solution of NaOH. The influence of temperature on ZnO NPs formation was studied by heating the solution on a water bath from 4°C - 90°C with constant stirring using a magnetic stirrer for 5 hours. The

colour changed from light orange to white, indicating the formation of ZnO NPs. The solution was cooled to 30 °C, purified by centrifugation at 1200 rpm for 6 minutes to obtain white precipitates. The precipitates were then washed four times with deionized water, dried for 24 hours at 90 °C and stored in a desiccator for further analysis.

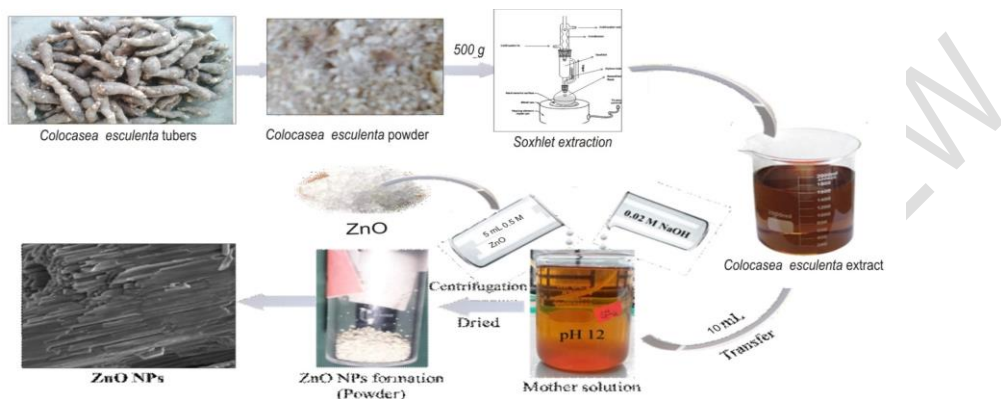


Figure 2: A modified schematic diagram for the preparation of ZnO NPs using *C esculenta* tuber peel extract (Farjana., et al, 2022).

2.5 CHARACTERIZATION OF ZNO NPS

The biosynthesized ZnO NPs were characterized by UV-visible spectroscopy, X-Ray Diffraction (XRD) analysis, Scanning Electron Microscopy (SEM), Energy Dispersive X-ray (EDX) and Fourier Transform Infrared (FTIR) spectroscopy. Uv-Visible spectrophotometer (Uv-3600 Plus, Shimadzu, Japan) in the range of 350-700 nm was used to confirm the formation of the ZnO NPs. Phase and unit cell dimension information was determined with the use of XRD-6000, Shimadzu, Japan with monochromatic Cu K α radiation (1.5419 Å), operated at 40 kV and 30 mA at 2 θ (25- 75°) and speed of 4° per minutes. SEM equipped with EDX (Philips XL-30, Eindhoven, Netherlands) was used to study the surface morphology and elemental composition of the ZnO NPs. FTIR analysis of the ZnO NPs was performed with Perkin Elmer FTIR Spectrophotometer-100 with the KBr pellet method in the range of 500 - 4000 cm⁻¹ to determine the functional groups responsible for the reduction of the Zn²⁺ as well as capping and stabilizing agents of the ZnO NPs.

2.6 ANTIMICROBIAL SENSITIVITY TEST

The method of (Shiriki., et al, 2017) was employed with slight modification. The biosynthesized ZnO NPs was tested against five previously isolated and identified white yam pathogenic fungi: *Aspergillus niger*, *Botryodiplodia theobromae*,

Zygosaccharomyces bailli, *Zygosaccharomyces rouxii* and *Myrothecium verrucaria* as well as three bacteria: *Klebsiella oxytoca*, *Serratia marcescens* and *Pseudomonas aeruginosa*. The pure isolates were individually cultured on ZnO NPs incorporated Potato Dextrose Agar (PDA) and Nutrient Agar (NA) plates for fungi and bacteria respectively and incubated at 37 °C for 7 days (fungi) and 24 hours (bacteria). Triplicates samples were prepared. The controls consisted of 1 mL 100 % fluconazol (200 mg) and 100 % of 1 mL ciprofloxacin (500 mg) tablets for fungi and bacteria respectively. Zone of inhibition (mm) where present was recorded with a transparent plastic ruler after the incubation period and the percentage inhibition zones calculated as follows:

$$\% \text{ Inhibition Zone (\% IZ)} = \frac{\text{Average diameter of pathogen colony}}{\text{Average diameter of pathogen in control}} \times 100 \% \dots\dots\dots(5)$$

The percentage inhibition was rated on the scale described by Sangoyemi (2004) as follows:

100 % inhibition (highly effective); 50 – 99 % inhibition (effective); 20 – 49 % inhibition (moderately effective); 0 – 19 % inhibition (slightly effective) and ≤ 0 % inhibition (not effective).

2.7 STATISTICAL ANALYSIS

The data obtained from the zone of inhibition (mm) was analyzed using one way analysis of variance (ANOVA). Differences between means were considered significant at $p < 0.05$.

3. RESULTS AND DISCUSSION

3.1 Phytochemical screening

Table 1 presents the result of the phytochemical analysis of *C. esculenta* tuber peel extract. The result indicated the presence of tannins, saponins, flavonoids, phenolics, alkaloids, steroids, starch, terpenoids and glycosides.

Table1. Phytochemical Analysis of *Colocasia esculenta* tuber peel extract

Secondary Metabolite	Test	Result
Tannins	FeCl ₃ Test	+
Saponins	Froth test	+
Flavonoids	Lead Acetate Test	+
Phenols	Ferric Chloride Test	+
Alkaloid	Hager's Test	+
Steroids	Libbermann Burchard's Test	+
Quinones	Hydrochloric Acid Test	-
Starch	Iodine Test	+
Terpenoids	Sakocoski's Test	+

Glycosides	Keller-Kallani's Test	+
------------	-----------------------	---

Key: + = positive, - = negative.

3.2 UV-VISIBLE SPECTROSCOPY ANALYSIS

The progress of the formation of ZnO NPs was followed by recording the absorption spectra as a function of time. The interaction between Zn²⁺ containing solution (ZnO) and the *C. esculenta* tuber peel extract shows λ_{max} at 365 nm with the absorption steadily building up with time and increasing temperature, reaching a maximum at 90 °C in five hours with a colour change from light orange to white, indicating the formation of ZnO NPs.

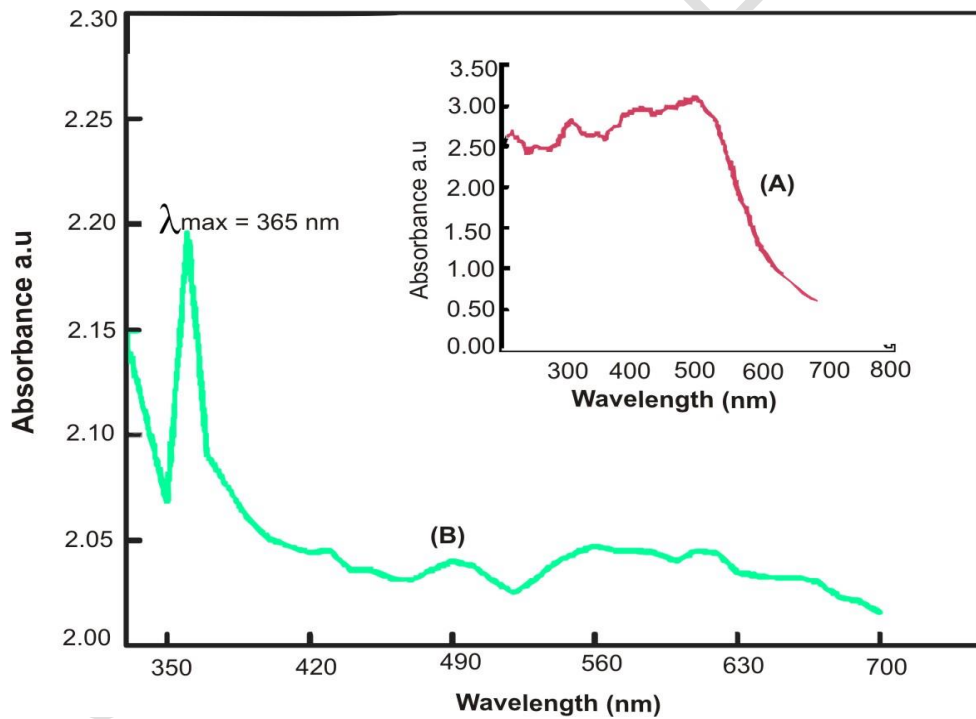


Figure 3: Uv-Vis spectra of (A) *Colocasia esculenta* tuber peel extract and (B) the biosynthesized ZnO NPs recorded as a function of reaction time.

3.3 X-RAY DIFFRACTION ANALYSIS

X-Ray diffraction is a non-destructive analytical method for the identification and quantitative determination of various crystalline forms (phases) and crystallite sizes of powder or solid samples. Diffraction occurs as the light waves interact with the regular structure whose repeated distance (d) is about the same as the wavelength (λ) according to the Bragg's equation:

$$n\lambda = 2d\sin\theta \dots\dots\dots(6)$$

Where λ = wavelength, d = interplaner spacing, θ = diffracted angle and n = , 1,2,3...

The biosynthesized ZnO NPs was subjected to XRD analysis.

UNDER PEER REVIEW

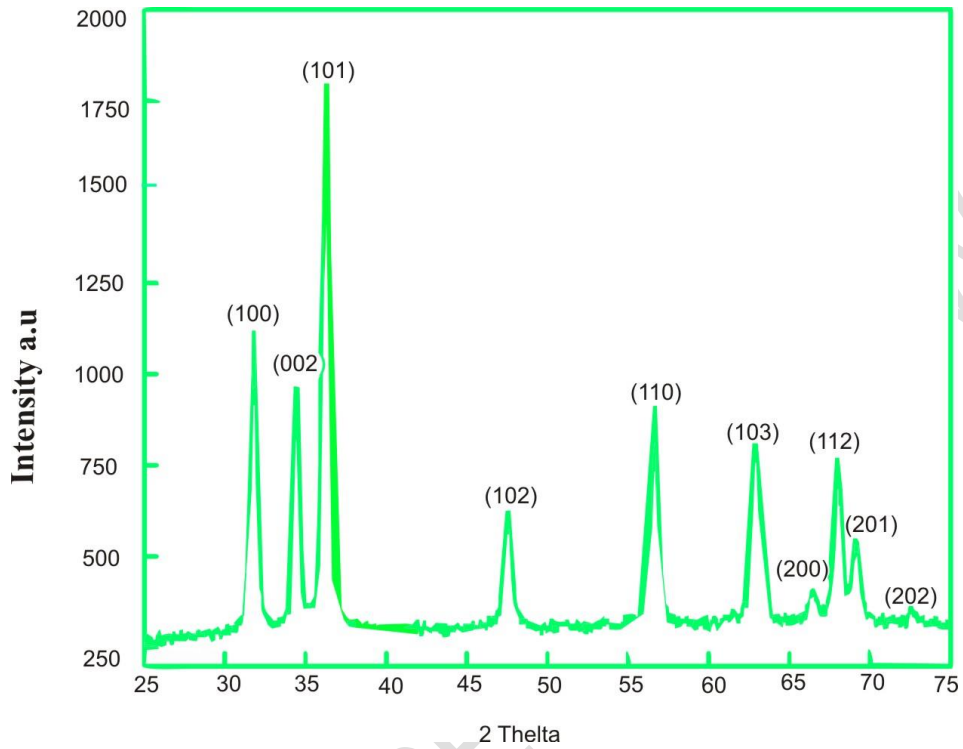


Figure 4: XRD pattern of the biosynthesized ZnO NPs.

Figure 4 represents the XRD spectra of the ZnO NPs. The XRD spectra revealed ten distinctive diffraction peaks at 2θ angles of 31.84° , 34.50° , 36.26° , 47.57° , 56.56° , 62.90° , 66.42° , 67.92° , 69.19° and 77.02° . Diffraction peaks are converted to d-spacing which is characteristic for each material that allow for the identification of the material. The diffracted peaks above can be assigned to miller indices of 100, 002, 101, 102, 110, 103, 200, 112, 201 and 202 respectively, corresponding to the reflection lines of hexagonal wurtzite structure according to the Joint Committee on Powder Diffraction Standards (JCPDS) card no: 36-1451 (Ramesh., et al, 2014).

The average crystallite size of the ZnO NPs was estimated by the Debye-Scherrer's equation

$$d = \frac{k\lambda}{\beta \cos \theta} \dots \dots \dots (7)$$

Where d = crystallite size (nm), k = correction/shape factor (0.9), β = full width at half maximum (FWHM) and θ = Bragg's angle (rad). The average crystallite size of the biosynthesized Zn NPs was calculated to be 10 nm with the range of 7.81 nm – 9.23 nm. A decreasing crystallite size leads to the broadening of the peak as peak width is inversely proportional to the crystallite size. The smaller the size, the narrower is the peak and vice versa.

3.4 SCANNING ELECTRON MICROSCOPY (SEM) WITH ENERGY DISPERSIVE X-RAY (EDX)

The scanning electron microscope (SEM) is a non-destructive method that uses accelerated and focused high-energy electrons to produce a variety of signals at the surface of solid samples because of electron-sample interactions. The size and surface morphology of the biosynthesized ZnO NPs was analyzed using SEM, while the elemental determination was carried out using energy dispersive X-ray (EDX). The SEM image of the ZnO is presented in Figure 5 which shows hexagonal shapes with good crystallinity.

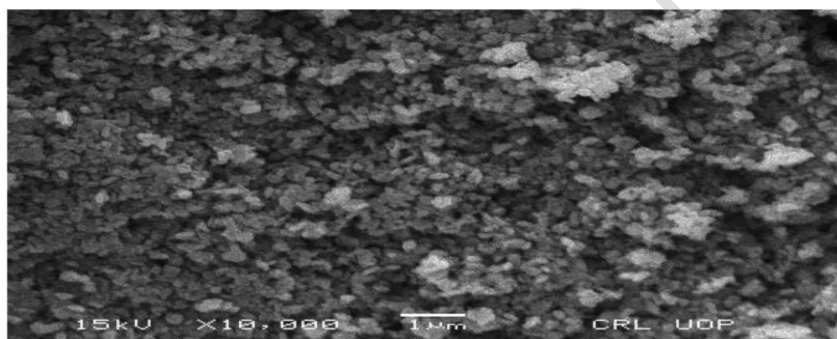


Figure 5. SEM image of biosynthesized ZnO NPs

pH strongly influences the degree of agglomeration, particle setting and size due to the change of surface charge and zeta potential of particles which allow for a greater degree of particle interaction. Generally, metal and metal oxide nanoparticles synthesis under acidic or neutral conditions tends to cause particle agglomeration. The optimal pH for the synthesis of ZnO NPs with lower agglomeration is 8 (Farjana et al., 2022). At low pH, the adsorption of metallic particles that were positively charged to negatively charged organic matter from capping agents is enhanced, resulting in higher degree of aggregation (Sibiya & Moloto, 2014). The acidic process would also change chemical structures and activities of the reductant to form alkoxide ions. Other studies (Sibiya & Moloto, 2014; Farjana. et al., 2022) confirmed that the size and density of the nanoparticles increase as a response to a decrease in the acidity of the medium. When the pH is

decreased continuously to a certain limits, it causes the re-dissolution of $Zn(OH)_2$, resulting in increased size (Farjan et al., 2022).

The calculation of the crystallite size of the ZnO NPs using ImageJ software gives the size of about 9.87 nm, which is in agreement with the calculated crystallite size of 10 nm from XRD data using the Debye-Scherrer equation. Hydrogen bonding and electrostatic interactions between biogenic capping molecules, and Nps cause agglomeration (Sibiya & Moloto, 2014). The SEM image shows that the ZnO NPs are not in direct contact with each other, signifying little agglomeration and the stabilization of ZnO NPs.

The elemental composition and purity of the ZnO NPs were determined by EDX analysis. Energy dispersive X-ray spectroscopy is an analytical technique used for the elemental analysis or chemical characterization and purity of a sample. The characterization capabilities are due in large part to the fundamental principle that each element has a unique atomic structure, allowing x-rays that are characteristic of an element's atomic structure to be identified uniquely from each other (Farjana et al., 2022).

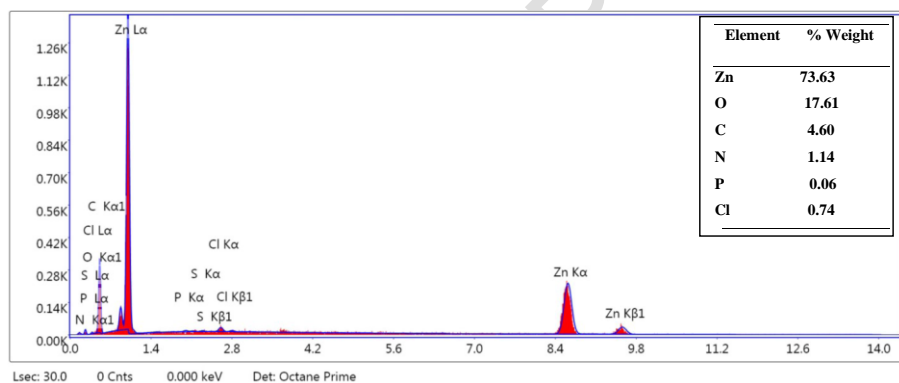


Figure 6: EDX spectrum of the biosynthesized ZnO

Figure 6 shows the chemical composition of the ZnO NPs with their respective percentages. The EDX spectrum shows characteristic peaks and elemental composition of Zn and Oxygen (73.63 %) and O (17.61 %) respectively, but low percentage of C, N, P, S and Cl which indicate high purity of the biosynthesized ZnO NPs.

3.5 FOURIER TRANSFORM INFRA-RED SPECTROSCOPY (FTIR) ANALYSIS

UNDER PEER REVIEW

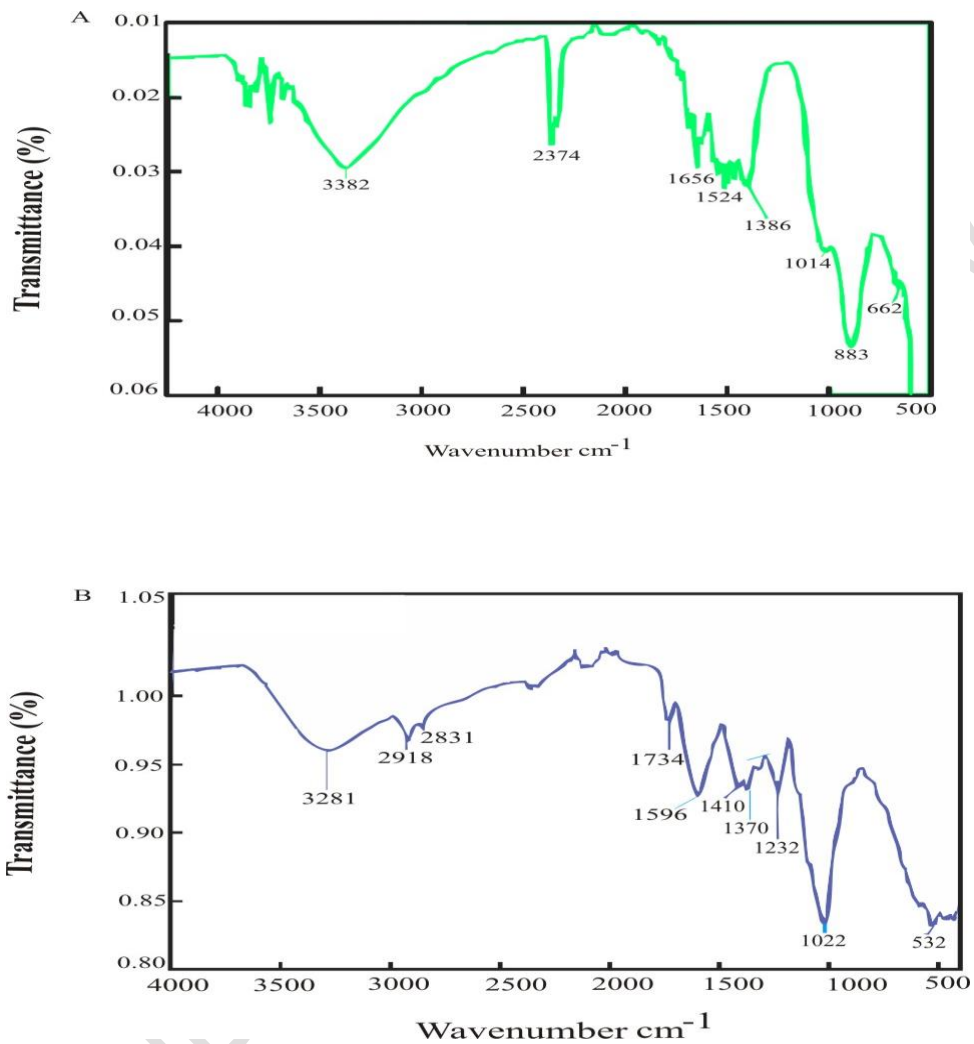


Figure 7: FTIR spectra of (A) the biosynthesized ZnO NPs and (B) *Cocosia. Esculenta* tuber pee extract.

The small peak at 662 cm^{-1} is allotted to the hexagonal wurtzite phase Zn-O stretching vibration. The broad peak at 3382 cm^{-1} is characteristic of stretching vibration of hydroxyl group (O-H) from polyphenols. The peak at 2374 cm^{-1} is attributed to the H-O-H vibrations of water molecules of crystallization. The peaks at 1656 cm^{-1} , 1524 cm^{-1} , 1380 cm^{-1} , 1014 cm^{-1} and 883 cm^{-1} are assigned to bending vibrations of C=C stretching of alkene, aromatic ring and polyphenols (C=O), C-H bending vibrations of alkane groups, stretching of C=N, and bending vibrations of C-H respectively.

The FTIR analysis of the *C. esculenta* tuber peel extract shows peaks at 3281 cm^{-1} which represents the symmetric O-H stretching, while that at 2918 cm^{-1} is assigned to phospholipids, cholesterol and creatine. The peak at 2831 cm^{-1} and 1734 cm^{-1} correspond to the C-H and C=O stretching respectively, while that at 1596 cm^{-1} represents C=N and NH_2 respectively. The peak at 1410 cm^{-1} is assigned to stretching C=N, N-H and C-H deformations. Peaks 1370 cm^{-1} corresponds to N-H deformation, while the peak at 1232 cm^{-1} is allocated to the overlapping of the protein amide III and the nucleic acid phosphate vibrations. The peaks at 1022 cm^{-1} and 532 cm^{-1} are assigned to the glycogen and sulphur compounds respectively.

The FTIR analysis confirmed the presence of functional groups from phytochemicals such as tannins, saponins, alkaloids, terpenes, flavonoids, phenols, steroids, and aromatic hydrocarbon, amines, amides etc which are responsible for the reduction of the Zn ions as well as capping and stabilizing agents of the ZnO NPs.

3.6 ANTIMICROBIAL STUDY OF THE ZNO NANOPARTICLES

The antimicrobial study of the ZnO NPs was carried out against five previously isolated and identified white yam pathogenic fungi: *Aspergillus niger*, *Botryodiplodia theobromae*, *Zygosaccharomyces bailli*, *Zygosaccharomyces rouxii* and *Myrothecium verrucaria* and three bacteria: *Klebsiella oxytoca*, *Serratia marcescens* and *Pseudomonas aeruginosa*. Table 2 represents the average zone of inhibition (mm), while Table 3 presents the percentage zone of inhibition (% IZ) of ZnO against the isolates.

Generally, the results showed that the inhibitory effects of the biosynthesized ZnO NPs increased with increasing concentration ($p < 0.05$). The biosynthesized ZnO NPs showed effective to slightly effective inhibition against the test organisms, ranging from 98.52 % - 15.54 % (Table 3). Effective inhibition (≥ 55.12 %), (≥ 60.64 %) and (≥ 53.55 %) against *Aspergillus niger*, *Zygosaccharomyces bailli* and *Zygosaccharomyces rouxii* respectively at all concentrations. The ZnO NPs was able to inhibit effectively *Botryodiplodia theobromae* (≥ 61.28 %) at all concentrations, except 10^{-3} , which exhibited moderately effective inhibition (38.72 %). *Myrothecium verrucaria* showed effective inhibition (≥ 70.00 %) at concentrations of 100 % and 10^{-1} %, while showing moderately effective inhibition (≥ 40.00 %) at 10^{-2} % and 10^{-3} %. Effective inhibition was recorded against *Klebsiella oxytoca* (≥ 70.31 %) at 100 % and 10^{-1} %, , while moderately effective inhibition (≥ 20.59 %) was obtained at ZnO NPs concentration of 10^{-2} %, 10^{-3} %.and 10^{-3} %. Effective (≥ 62.16 %), moderately effective (21.52 %) and slightly effective (15.54 %) inhibitions were recorded at 100 %, 10^{-1} %, 10^{-2} % and 10^{-3} % respectively against *Serratia marcescens*. *Pseudomonas aeruginosa* was effectively inhibited (≥ 53.27 %) at 100 %, 10^{-1}

% and 10^{-2} %, but moderately (25.76 %) inhibited at 10^{-3} . The results are comparable with standard antimicrobial agents: fluconazole and ciprofloxacin ($p > 0.05$).

Table 2: Antimicrobial Sensitivity Test/ Average Zone of Inhibition (mm) of Biosynthesized ZnO NPs

Isolates	Zinc Oxide Nanoparticles Concentration (%)				Control
	100	10^{-1}	10^{-2}	10^{-3}	
Fungi					
<i>Aspergillus niger</i>	8.33 ± 0.82	7.83 ± 0.99	7.00 ± 0.63	5.33 ± 0.52	9.67 ± 2.69
<i>Botryodiplodia theoromae</i>	8.33 ± 0.82	7.50 ± 0.54	6.33 ± 0.51	4.00 ± 4.38	10.33 ± 1.96
<i>Zygosaccharomyces bailli</i>	8.33 ± 0.82	7.50 ± 0.54	7.00 ± 0.63	6.67 ± 0.32	11.00 ± 0.89
<i>Zygosaccharomyces rouxii</i>	10.67 ± 3.00	8.16 ± 0.98	7.50 ± 0.55	5.80 ± 0.41	10.80 ± 0.98
<i>Myrothecium verrucaria</i>	26.83 ± 12.98	21.0 ± 4.05	13.00 ± 2.19	12.00 ± 2.19	30.00 ± 6.03
Bacteria					
<i>Klesiella oxytoca</i>	30.00 ± 4.60	15.67 ± 5.61	9.00 ± 2.37	7.17 ± 1.17	34.83 ± 0.75
<i>Serratia marcescens</i>	43.84 ± 1.72	26.00 ± 0.89	9.00 ± 3.4	6.50 ± 1.05	41.83 ± 3.31
<i>Pseudomonas aeruginosa</i>	37.16 ± 3.37	26.83 ± 4.67	20.33 ± 1.63	9.83 ± 2.79	38.16 ± 3.87

N= 6, values expressed as Mean ± SD.

Table 3. Percentage Zone of Inhibition of the Isolates to Different Concentrations of the Biosynthesized Zn NPs

Microorganism	Concentration (%)			
	100	10 ⁻¹	10 ⁻²	10 ⁻³
Fungi				
<i>Aspergillus niger</i>	86.14	80.97	72.39	55.12
<i>Botryodiplodia theobromae</i>	80.64	72.60	61.28	38.72
<i>Zygosaccharomyces bailli</i>	75.73	68.18	63.64	60.64
<i>Zygosaccharomyces rouxii</i>	98.52	75.35	69.25	53.55
<i>Myrothecium verrucaria</i>	89.43	70.00	43.33	40.00
Bacteria				
<i>Klebsiella oxytoca</i>	86.13	70.31	45.04	20.59
<i>Serratia marcescens</i>	83.27	62.16	21.52	15.54
<i>Pseudomonas aeruginosa</i>	97.37	70.31	53.27	25.76

CONCLUSION

ZnO NPs was successfully prepared using *C. esculenta* tuber peel extract through green route method. The biosynthesized ZnO NPs was characterized by UV-Vis, XRD, EDX, SEM and FTIR analysis. UV-Vis analysis confirmed the formation of ZnO NPs at 365 nm with the hexagonal wurtzite shape and average crystallite size of 10 nm, ranging from 7.81 nm to 9.23 nm. Elemental analysis from EDX confirmed high percentage weight of Zn and O, but lower percentages of C, N, P, S and Cl, indicating high purity of the biosynthesized ZnO NPs. The FTIR analysis confirmed the presence of organic functional groups responsible for the reduction, capping and stabilization of the ZnO NPs. The antimicrobial study of the ZnO NPs against eight white yam pathogens compared favourably with standard antifungal (fluconazole) and antibacterial (ciprofloxacin) agents. The biosynthesized ZnO NPs holds great potential to providing effective solutions to the multiple agricultural-related problems, including yam tuber rot control and can provide an alternative to synthetic antimicrobial agents since it is less expensive, environmentally friendly, biocompatible and easy to prepare.

REFERENCES

- Amin, G., Asif, M .H, Zainelabidin, A., Zaman, S., Nur, O, and Willander, M. (2011). Influence of pH, precursor concentration, growth time, and temperature on the morphology of ZnO nanostructures grown by the hydrothermal method *Journal of nanomaterials* 269692.
- Divya, M.J., Sowmia, C., Joona, K., Dhanya, K.P. (2013). Synthesis of zinc oxide nanoparticle from Hibiscus rosa-sinensis leaf extract and investigation of its antimicrobial activity. *Res.*

Commented [2A4]: References shall be uniform.

Eleazu, C.O. (2016). Characterization of the natural products in cocoyam (*Colocasia esculenta*) using GC-MS. *Pharmaceutical Biology*, 54 (12), 2880-2885.

Elumalai, K, and Velmurugan S. (2015). Green synthesis, characterization and antimicrobial activities of zinc oxide nanoparticles from the leaf extract of *Azadirachta indica* (L) *Applied Surface Science* 345 329-36.

Farjana R., Md Abdul M. P., Md. Abu, B. S., Muhammad, S.B., Md. Aminul H., Beauty, A., Rimi R., Md. Anamul H., Royhan, A. K. M. (2022). A Green synthesis of ZnO nanoparticles using *Cocos nucifera* leaf extract: Characterization, antimicrobial, antioxidant, and photocatalytic activity. <https://doi.org/10.1101/2020.10.27.514023>.

Gunalan, S., Sivaraj, R., and Rajendran, V. (2012). Green synthesized ZnO nanoparticles against bacterial and fungal pathogens. *Prog. Nat. Sci. Mater. Int.* 22 (6), 693–700, [org/10.1016/j.pnsc.2012.11.015](https://doi.org/10.1016/j.pnsc.2012.11.015). *J. Pharm. Biol. Chem.* 4 (2), 1137–1142

Jayanta, K.B. (2020). Synthesis and Characterization of ZnO Nanoparticles. A Master of Science Dissertation of the Department of Physics, National Institute of Technology, Rourkela, Orissa, India.

Jha, A.K., Kumar, V., Prasad, K. (2011). Biosynthesis of metal and oxide nanoparticles using orange juice. *J. Bionanosci.* 5 (2), 162–166. <http://dx.doi.org/10.1166/jbns.2011.1053>.

Josef, J., & Katarina, K. (2015). Application of Nanotechnology in Agriculture and Food Industry, its Prospects and Risks. *Ecol CHEM ENG S.*, 22(3), 321-361.

Kharisova, O.V., Dias, H.V R., Kharisov, B.I., Perez, B.O, and Perez, V.M .J (2013). The greener synthesis of nanoparticles *Trends in Biotechnology* 31(4) 240-48

Lakshmi, J.V., Sharath, R., Chandraprabha, M.N., Neelufar, E., Hazra, Abhishikta, Patra, Malyasree. (2012). Synthesis, characterization and evaluation of antimicrobial activity of zinc oxide nanoparticles. *J. Biochem. Technol.* 3 (5), S151–S154.

Liu, J., Burdette, J.E., Xu, H., Gu, C., van Breemen, R.B., Bhat, K.P., Booth, N., Constantinou, A.I., Pezzuto, J.M., Fong, H.H., Farnsworth, N.R., Bolton, J.L. (2001). Evaluation of estrogenic activity of plant extracts for the potential treatment of menopausal symptoms. *J. Agric. Food Chem.* 49, 2472–2479.

Mittal A K., Chisti, Y, and Banerjee, U.C. (2013). Synthesis of metallic nanoparticles using plant extracts *Biotechnol Adv* doi: 10.1016/j.biotechadv.2013.01.003.

Moloto, N., Revaprasadu, N., Musetha, P.L, and Moloto, M.J. (2009). The effect of precursor concentration, temperature and capping group on the morphology of CdS nanoparticles *Journal of Nanoscience and Nanotechnology* 9:4760-66.

Nakade, D.B., Mahseh, S.K., Kiran, N.P, and Vinayak, S.M. (2013). Phytochemical screening and Antibacterial Activity of Western Region wild leaf *Colocasea esculenta*. *International Research Journal of Biological Science* 2 (10): 1-6.

Padil, V.V., T and Cernik, M. (2013). Green synthesis of copper oxide nanoparticles using gum karaya as biotemplate and their antibacterial application *International Journal of Nanomedicine* 8 889-98.

Parveen, K., Banse, V, and Ledwani, L. (2016). Green synthesis of nanoparticles: their advantages and disadvantages *2nd International Conference on Emerging Technologies: micro to nano 2015 (ETMN-2015)* doi: 10.1063/1.4945168

Pritha, C., Papiya, D., Sudeshna, C., Bohniskilda, C, and Jayantihi, A. (2015). Cytotoxicity and antimicrobial activity of *Colocasea esculenta*. *Journal of Chemical and Pharmaceutical Research*, 7(12): 627-635.

Rajiv, P., Rajeshwari, S., Venckatesh, R. (2013). Rambutan peels promoted biomimetic synthesis of bioinspired zinc oxide nanochains for biomedical applications. *Spectrochim. Acta Part A Mol. Biomol. Spectros.* 112, 384–387. <http://dx.doi.org/10.1016/j.saa.2014.08.022>.

Ramesh, P., Rajendran, A., Meenakshisundaram, M., 2014. Greensynthesis of zinc oxide nanoparticles using flower extract *Cassia Auriculata*. *J NS NT* 1 (1), 41–45, February |Pp 41- 45| ISSN 2279 –0381.

Salam, A.H., Sivaraj, R., Venckatesh, R. (2014). Green synthesis and characterization of zinc oxide nanoparticles from *Ocimum basilicum* L. var. *purpurascens* Benth.-Lamiaceae leaf extract. *Mater. Lett.* 131, 16–18. <http://dx.doi.org/10.1016/j.matlet.2014.05.033>.

Sangeetha, G., Rajeshwari, S., Venckatesh, R. (2011). Green synthesis of zinc oxide nanoparticles by aloe *barbadensis* miller leaf extract: structure and optical properties. *Mater. Res. Bull.* 46: 2560–2566.

Sathishkumar, G., Rajkuberan, C., Manikandan, K., Prabukumar, S., Daniel John, J., Sivaramakrishnan, S. (2017). Facile biosynthesis of antimicrobial zinc oxide (ZnO) nanoflakes using leaf extract of *Couroupita guianensis*. *Aubl. Mater. Lett.* 188: 383–386.

Shiriki, D., Obochi, G.O., Eke, M.O, and Shambe, T (2017). Postharvest Loss Control: Synergistic Plants Extract Inhibition of Ten Microbial Yam Rot Organisms, , 8, 7 25-732. <https://doi.org/10.4236/fns.2017.87051>

Shiriki, D., Ubwa, S.T., Yusufu, M.I and Shambe, T. (2019). Extraction methods and inhibition studies of Ten plant extracts on nine Yam Rot Pathogenic Microorganisms. *Food and Nutrition Sciences.* <https://doi.org/10.4236/fns.2019>.

Sibiya, P.N, and Moloto, M.J. (2014). Effect of precursor concentration and pH on the shape and size of starch capped silver selenide (Ag₂Se) nanoparticles *Chalcogenide Letters* 11(11) 577- 88.

Vijayakumar, S., Vinoj, G., Malaikozhundan, B., Shanthi, S., Vaseeharan, B. (2015). *Plectranthus amboinicus* leaf extract mediated synthesis of zinc oxide nanoparticles and its control of methacillin resistant *Staphylococcus aureus* biofilm and blood sucking mosquito larva. *Spectrochim. Acta Part A Mol. Biomol. Spectrosc* 137: 886-891. <http://dx.doi.org/10.1016/j.saa.2014.08.064>.

Wang, J.K. (2012). Taro-a review of *Colocasia esculenta* and its potentials. . *Journal of Biotechnology and Pharmaceutical Research* 3, 42-46.

Yasser, S, and Nassim, S. (2019). Current advances in applications of chitosan based nano metal oxides as food preservative materials. *Nanomed J* 4(): 122-129.

Zare, E., Pourseyedi, S., Khatami, M ,and Darezereshki, E. (2017). Simple biosynthesis of zinc oxide nanoparticles using nature's source, and its in vitro bio-activity *Journal of Molecular Structure* 1146 96-103.